

1 **Regionalized life cycle assessment of present and future lithium**  
2 **production for Li-ion batteries**

3 **Authors:** Vanessa Schenker<sup>1,2</sup>, Christopher Oberschelp<sup>1,2</sup>, Stephan Pfister<sup>1</sup>

4 **Affiliations:**

5 <sup>1</sup> Institute of Environmental Engineering, ETH Zürich, John-von-Neumann-Weg 9, 8093 Zürich,  
6 Switzerland

7 <sup>2</sup> National Centre of Competence in Research (NCCR) Catalysis, ETH Zürich, Zürich, Switzerland

8 **Corresponding author:** Vanessa Schenker, [vanessa.schenker@ifu.baug.ethz.ch](mailto:vanessa.schenker@ifu.baug.ethz.ch), twitter: @schvanes

9 **Contacts of co-author:** Dr. Christopher Oberschelp, [christopher.oberschelp@ifu.baug.ethz.ch](mailto:christopher.oberschelp@ifu.baug.ethz.ch)

10 **Contacts of co-author:** Dr. Stephan Pfister, [stephan.pfister@ifu.baug.ethz.ch](mailto:stephan.pfister@ifu.baug.ethz.ch)

11 This paper is a non-peer reviewed preprint submitted to EarthArXiv. This study has been submitted for  
12 peer-review and publication in Resources, Conservation and Recycling.

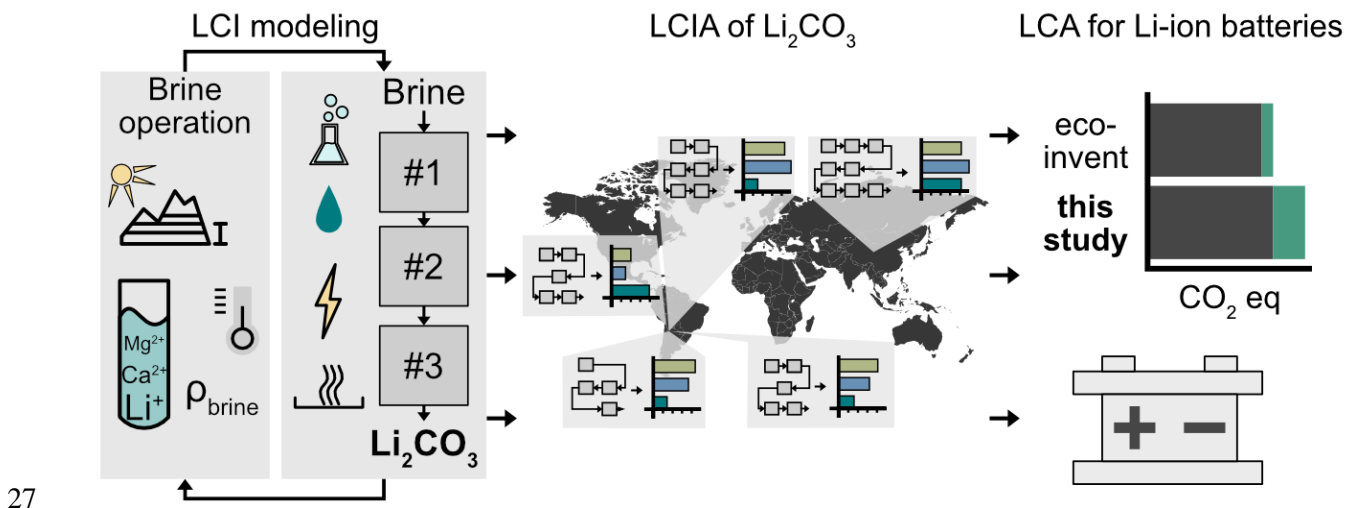
13

14 **Abstract**

15 Existing life cycle assessments (LCA) of lithium carbonate production from brines are mainly based on one  
16 single brine operation site, while many different lithium carbonate production routes have been developed  
17 in the past. Hence, current life cycle inventories do not capture the variability of brine sites and misestimate  
18 life cycle impacts. This study presents a systematic approach for LCA of existing and future lithium  
19 carbonate production from brines, which can furthermore be applied to geothermal brines or seawater. It  
20 has been used to model life cycle inventories of three existing and two upcoming brine operations in  
21 Argentina, Chile, and China and combined with regionalized life cycle impact assessment. Impacts on  
22 climate change, particulate matter human health impacts, and water scarcity from lithium carbonate  
23 production differ substantially among sites. Existing life cycle inventories for lithium-ion battery  
24 production underestimate climate change impacts by up to 19% compared to one from our study.

25 **Keywords:** Lithium, Environmental impacts, Life cycle assessment, Life cycle inventory, Brines

26 **Graphical abstract**



## 28 **1 Introduction**

29 The development of energy storage led to an increased demand for battery metals (Christmann et al., 2015;  
30 Wanger, 2011; World Economic Forum, 2019). By 2030, the battery demand is forecasted to grow by 1400  
31 % and hence, the demand for Lithium (Li) used in Li-ion batteries is expected to increase by a factor of 6  
32 with respect to 2018 (World Economic Forum, 2019).

33 More than two-thirds of the Li resources are located in Argentina, Bolivia, Chile, and China as brine  
34 deposits which hold a great supplying potential in the future (Bertau et al., 2017; Kesler et al., 2012; Munk  
35 et al., 2016). The primary producer of lithium carbonate ( $\text{Li}_2\text{CO}_3$ ) from brines is Chile, followed by  
36 Argentina and China (S&P Global, 2021). Brine operations produce  $\text{Li}_2\text{CO}_3$  with a technical grade (min.  
37 99 wt. %) and battery grade (99.5 wt. %). The latter is used to manufacture Li-ion batteries (Dai et al.,  
38 2020).

39 Various production routes for  $\text{Li}_2\text{CO}_3$  from brines have been developed in the past (Tran and Luong, 2015).  
40 Generally, the processing can be subdivided into three main processes: Brine's mass reduction in solar  
41 evaporation ponds, brine purification, and  $\text{Li}_2\text{CO}_3$  precipitation (Garrett, 2004; Tran and Luong, 2015). The  
42 brine is pumped from an aquifer/salt lake into evaporation ponds to reduce the brine volume by solar  
43 evaporation. When a specific Li concentration of the brine is reached, the brine is sent to the processing  
44 plant. The purification part consists of a variety of processes in different arrangements to remove impurities  
45 (Calcium (Ca), magnesium (Mg), or boron (B)) from the Li-enriched brine, such as by adding quicklime to  
46 remove Mg, using organic solvent extraction to remove B, or using ion exchangers to remove Mg, Ca, or  
47 B. The selected processes and their order depend on the site-specific brine compositions. Once the pulp has  
48 been purified,  $\text{Li}_2\text{CO}_3$  is precipitated by heating the pulp and adding soda ash. Crystallized  $\text{Li}_2\text{CO}_3$   
49 (technical grade) is dissolved in water at low temperature. The solution is re-heated at 80 °C, and  $\text{Li}_2\text{CO}_3$   
50 (battery grade) precipitates. The final product is dried in a rotary dryer (Garrett, 2004; Tran and Luong,  
51 2015). In addition to this approach of extracting Li from brines, other processing techniques include  
52 selective Li recovery. The Li-ion selective adsorption technique uses adsorbents (manganese oxide,

53 titanium oxide, or alumina) to selectively uptake Li from the brine sent through the ion exchangers (Garrett,  
54 2004; Tran and Luong, 2015). Once the adsorbents are saturated with Li, the columns are washed and take  
55 up Li. The Li-containing solution is then sent to evaporation ponds to further concentrate Li (Garrett, 2004).  
56 Once a specific concentration is reached in the solution,  $\text{Li}_2\text{CO}_3$  precipitation (technical grade) is forced by  
57 heating the pulp and adding soda ash, as explained for the previous production route. Crystallized  $\text{Li}_2\text{CO}_3$   
58 (technical grade) is dissolved in water at low temperature by adding pressurized gaseous  $\text{CO}_2$ . The solution  
59 is re-heated at 80 °C, and  $\text{Li}_2\text{CO}_3$  (battery grade) precipitates. The product is dried in a rotary dryer (Garrett,  
60 2004; Tran and Luong, 2015).

61 Regarding environmental impacts, energy provision for  $\text{Li}_2\text{CO}_3$  production is mainly based on fossil fuels  
62 contributing to climate change (Stamp et al. 2012, Kelly et al. 2021). Stamp et al. (2012) published life  
63 cycle inventory (LCI) data for brine-related  $\text{Li}_2\text{CO}_3$  production from the Salar de Atacama in Chile. This  
64 data was integrated into the ecoinvent LCI database in 2012 and has not been updated or expanded  
65 (ecoinvent, 2021). Kelly et al. (2021) used more updated recent technical data from the Salar de Atacama  
66 to quantify impacts on climate change and water scarcity but also did not improve on the coverage in terms  
67 of different sites. Ambrose and Kendall (2019) slightly extended the coverage by including lab-scale data  
68 from the Salar de Uyuni in Bolivia when assessing climate change impacts.

69 When assessing water scarcity impacts related to Li-ion battery storage, water scarcity impacts of Li from  
70 brines were classified as critical, according to Schomberg et al. (2021). They included brine consumption  
71 in the water scarcity footprint (WSF) when applying the LCA midpoint indicator AWARE. However, brines  
72 are not directly used by ecosystems or humans as a water source and should, thus, not be considered when  
73 applying this LCA method (Boulay et al., 2018). Brine pumping affects the hydrogeological systems with  
74 wetland and lake ecosystems at the Salar de Atacama but these direct and indirect effects of brine pumping  
75 are only measurable by assessing the hydrogeology of these salt flats (Liu et al., 2019; Liu and Agusdinata,  
76 2021; Marazuela et al., 2019).

77 The scientific focus has been LCIs of  $\text{Li}_2\text{CO}_3$  production from Salar de Atacama in Chile so far (57 % of  
78 the LCE production from brines in 2018 (S&P Global, 2021)). However, processing techniques from other  
79 brine operations differ from the one used at Salar de Atacama since they vary in their chemical composition  
80 (Flexer et al., 2018; Houston et al., 2011; Munk et al., 2016; Tran and Luong, 2015). Thus, production  
81 routes adapted to the brine chemistry and other environmental parameters were developed (Garrett, 2004;  
82 Swain, 2017; Tran and Luong, 2015). Hence, what is missing so far in literature is a detailed assessment of  
83 other  $\text{Li}_2\text{CO}_3$  production pathways and their related environmental impacts. Furthermore, the existing LCA  
84 studies are difficult to compare since the goal and scope of these studies vary. Differences in system  
85 boundaries and degree of transparency hamper the direct comparison of these studies. Hence, the main  
86 objective of this paper is to develop a systematic approach to model site-specific LCIs of  $\text{Li}_2\text{CO}_3$  production  
87 from brines when operational data from the companies are not publicly available. We apply our approach  
88 by assessing environmental impacts of  $\text{Li}_2\text{CO}_3$  (battery grade) production from five brine operations in  
89 Chile, Argentina, and China. We cover climate change impacts, regionalized human health impacts from  
90 fine particulate matter (PM) formation and partly regionalized WSFs. Finally, by integrating  $\text{Li}_2\text{CO}_3$  from  
91 different brine operations, the consequences on climate change impacts related to Li-ion battery production  
92 were assessed.

## 93 **2 Methods**

### 94 **2.1 Framework to assess environmental impacts of $\text{Li}_2\text{CO}_3$ from brines**

95 We present an approach to quantify environmental impacts of  $\text{Li}_2\text{CO}_3$  production from brines. Specifically,  
96 we developed a modular approach to model site-specific LCIs, which allows for flexible adjustments to  
97 future process updates at each extraction site and can also be applied to other brines in future research. The  
98 approach follows the ISO 14040:2006 and ISO 14044:2006 standards to allow a standardized LCA (ISO,  
99 2006a, 2006b). Hence, four steps need to be examined: Goal and scope definition, LCI analysis, life cycle  
100 impacts assessment, and the final interpretation.

101 **Step 1: Goal and scope**

102 The goal and scope should be defined in the first step. We suggest setting the functional unit to 1 kg  $\text{Li}_2\text{CO}_3$   
103 (battery grade) which facilitates the integration of LCIs in Li-ion batteries. System boundaries should be  
104 set accordingly to the project's scope (e.g., the system boundaries (cradle-to-gate approach) could be set  
105 from pumping the brines to the surface until the final product ( $\text{Li}_2\text{CO}_3$ , battery grade) leaves the processing  
106 plant).

107 **Step 2: LCI analysis**

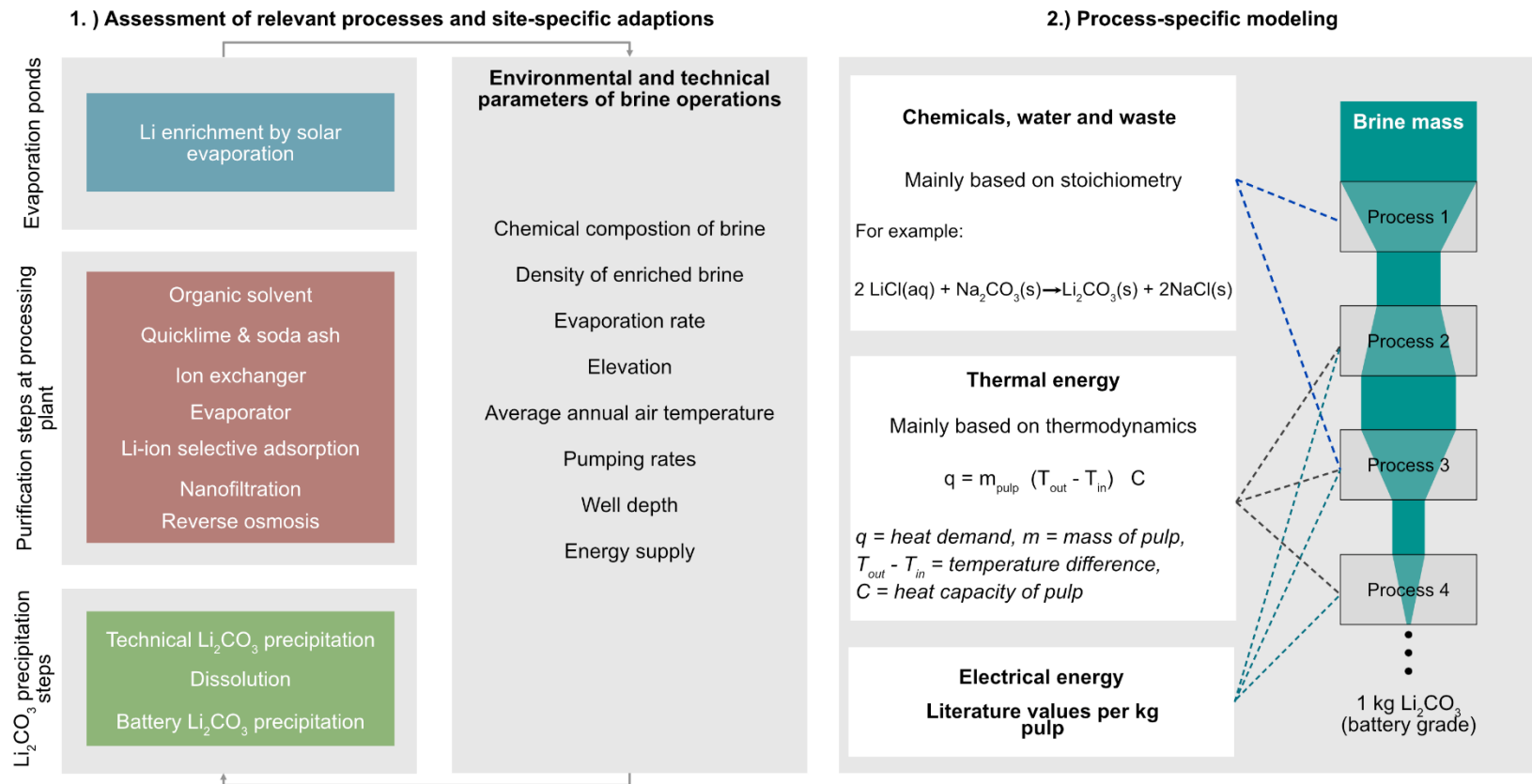
108 Step 2 consists of modeling the LCI for  $\text{Li}_2\text{CO}_3$  production from one or multiple brine sites if site data are  
109 not publicly available. We propose using the approach as developed in this study (Figure 1): (1)  
110 identification of relevant processes and site-specific environmental and technical parameters and (2)  
111 process-specific modeling of energy and material demand.

112 **(1) Identification of relevant processes and site-specific parameters**

113 Literature research (e.g., company reports, patents, scientific papers) is required to identify the relevant  
114 processes to produce  $\text{Li}_2\text{CO}_3$ . The process configuration determines the mass flows of the Li-containing  
115 pulp and thus, requires a detailed assessment for the latter LCI modeling. The types of input and waste  
116 production for all identified processes need to be defined. Environmental and technical parameters (e.g.,  
117 chemical composition of the brine, evaporation rate, or annual average air temperature) need to be  
118 considered because they influence resource demand of  $\text{Li}_2\text{CO}_3$  production (e.g., heating demand of  $\text{Li}_2\text{CO}_3$   
119 precipitation or the chemical demand to remove B from the pulp). Sources of thermal energy can be  
120 retrieved from company reports. Identifying processes and relevant parameters is an iterative process since  
121 the type of  $\text{Li}_2\text{CO}_3$  production also guides the number and type of parameters required for LCI modeling.

122       **(2) Process-specific modeling of material and energy demand**

123       The reported Li concentration of the enriched brine serves as an approximation for the required mass of  
124       brine entering the processing plant. The input demand for processes, such as purification (Mg removal by  
125       adding quicklime) and  $\text{Li}_2\text{CO}_3$  precipitation (adding soda ash), is dependent on the mass flows (pulp  
126       entering the process). The chemical composition of the brine affects required industrial chemical demand  
127       (e.g., the mass of Mg in the brine is proportional to the amount of quicklime if it is added to brine stored in  
128       the evaporation ponds (Flexer et al. 2018)). Mass of process-related chemicals (e.g., quicklime to remove  
129       Mg in the pulp) and produced waste (e.g., NaCl precipitation due to soda ash) are suggested to be  
130       stoichiometrically calculated. The required mass of chemicals should be adapted by adding a percentage to  
131       account for the incompleteness of chemical reactions according to available data. Those inputs and outputs  
132       need to be investigated to determine the mass of pulp going into the next process. Further affecting mass  
133       flows within the processing plant is residual pulp re-circulation to previous purification steps, which needs  
134       to be considered if reported. Energy demand can be quantified once process-specific mass flows are  
135       determined. Thermal energy demands are influenced by the mass, temperature difference, and heat capacity  
136       of the pulp (Figure 1). Literature values per kg pulp for process-specific electricity demands are available  
137       and can be used to determine the operational electricity requirement on-site.



138

139 *Figure 1: Proposed approach to model LCI for Li<sub>2</sub>CO<sub>3</sub> production from brines.*

140

### 141 **Step 3a: Life cycle impact assessment**

142 To assess environmental impacts of  $\text{Li}_2\text{CO}_3$  (battery grade) production from each brine operation, we  
143 suggest to consider impacts on climate change (GWP 100a) (IPCC 2013), fully regionalized LCA impact  
144 assessment of fine PM formation (Oberschelp et al. 2020), and partly regionalized WSF based on AWARE  
145 (Boulay et al., 2018). The selection of impact categories (impacts on climate change and water scarcity) is  
146 based on existing literature (e.g., Stamp et al. 2012; Schomberg et al. 2021; Kelly et al. 2021). Since the  
147 energy requirement is mainly based on fossil fuels (Kelly et al., 2021), PM-related human health impacts  
148 should also be assessed, as it was shown in Oberschelp et al. (2019).

### 149 **Step 3b: Sensitivity analyses**

150 Monte Carlo simulations for brine operations allow to analyze the robustness of the results. Uncertainty  
151 distribution types (e.g., triangular or log-normal distributions) need to be carefully chosen. If many data are  
152 available, a random sampling of several datasets should be performed. Changing parameters based on  
153 physical relations could be a less preferred option to test the results. For the case of limited data, the data  
154 quality should be expressed by the Pedigree matrix described in Wernet et al. (2016).

## 155 **3 Results and discussion**

### 156 **3.1 Application of the approach to present and future brine sites**

157 To test our presented framework, the lithium extraction sites (Salar de Atacama, Salar de Olaroz, Salar de  
158 Cauchari-Olaroz, Salar del Hombre Muerto (North), Chaerhan salt lake) were environmentally assessed.  
159 Of the five selected sites, Salar de Atacama, Salar de Olaroz, and Chaerhan salt lake have been producing,  
160 whereas Salar de Cauchari-Olaroz is currently in the construction phase and plans to start  $\text{Li}_2\text{CO}_3$   
161 production in 2022 (S&P Global, 2021) while Salar del Hombre Muerto (North) is at an early exploration  
162 stage. For the latter, the start of mining activity and extraction technology is not yet clearly set (S&P Global,

163 2021), but a  $\text{Li}_2\text{CO}_3$  production pathway has been suggested by Knight Piésold Ltd. and JDS Energy &  
164 Mining Inc. (2019).

165 This paper covers 70 % of the brine-related lithium carbonate production worldwide (sum of current  
166 production from the Salar de Atacama, Salar de Olaroz, and Chaerhan salt lake) (S&P Global, 2021). We  
167 also cover future production sites at Salar de Cauchari-Olaroz and Salar del Hombre Muerto North (reported  
168 and estimated production given in Table 1).

### 169 **Step 1: Goal and scope**

170 The goal is to quantify environmental impacts of  $\text{Li}_2\text{CO}_3$  (battery grade) production from brine operations  
171 and to allow a comparison among them using an attributional LCA with the cut-off allocation approach  
172 from ecoinvent (Wernet et al., 2016). The functional unit was 1 kg  $\text{Li}_2\text{CO}_3$  (battery grade). We used a  
173 cradle-to-gate approach. The system boundaries from pumping the brine to the surface until the final  
174 product ( $\text{Li}_2\text{CO}_3$ , battery grade) leaves the processing plant for the South American salt lakes. At Chaerhan  
175 salt lake, the brine is first sent to a K-fertilizer plant, and  $\text{Li}_2\text{CO}_3$  production uses the effluent, which is  
176 considered as a waste stream and, therefore, without burden in the cut-off allocation approach. Since only  
177  $\text{Li}_2\text{CO}_3$  (technical grade) is produced (Gansu United testing services Co Ltd (2018), Lanke Lithium (2018)),  
178 we added the processes (dilution and re-heating the Li-bearing solution) required to manufacture  $\text{Li}_2\text{CO}_3$   
179 (battery grade). We further assessed the environmental impacts of Li-ion battery production. We  
180 incorporated our modeled LCIs of Chaerhan salt lake and Salar de Atacama in the Li-ion battery production  
181 based on ecoinvent v3.8 cut-off (ecoinvent, 2021). The functional unit was 1 kg of rechargeable Li-ion  
182 battery. Brightway 2 by Mutel (2017) and Activity Browser by Steubing et al. (2020) were used to conduct  
183 the assessment.

184 **Step 2: LCI analysis**

185 **(1) Identification of relevant processes and parameters**

186 We identified the relevant processes and their input demand for the chosen brine sites (Table 1, graphical  
187 illustration Figure 2). Required environmental and technical parameters are presented in the SI for each  
188 brine operation. Salar de Atacama, Salar de Cauchari-Olaroz, and Salar del Hombre Muerto (North) have  
189 similar general  $\text{Li}_2\text{CO}_3$  production routes but with varying purification steps. While Salar de Olaroz uses  
190 ion exchangers to remove impurities from the pulp, Chaerhan salt lake uses Li-ion selective ion exchangers  
191 to adsorb Li.

192 *Table 1 Differences in main processing techniques for the investigated brine operations. Production in metric tons of*  
193 *Salar de Atacama, Salar de Olaroz, and Chaerhan salt lake for the year 2018 are based on S&P Global (2021).*  
194 *Estimated production at Salar de Cauchari-Olaroz is given by Andeburg Consulting Services Inc and Montgomery &*  
195 *Associates (2019) and at Salar del Hombre Muerto (North) by Knight Piésold Ltd. and JDS Energy & Mining Inc.,*  
196 *(2019).*

<b>Brine operation</b>	<b>Processing techniques</b>
Salar de Atacama, Chile (88 100 t $\text{Li}_2\text{CO}_3$ )	The brine is pumped into evaporation ponds to enrich Li from 0.15 wt. % to 6 wt. % and then transported to the processing plant (Garrett 2004). Subsequently, purification steps consist of organic solvent extraction to remove B and adding quicklime, respectively soda ash to remove Mg and Ca (Wilkomirsky, 1999). Then soda ash is added to the heated brine to let $\text{Li}_2\text{CO}_3$ (technical grade) precipitate (Kelly et al., 2021; Wilkomirsky, 1999). $\text{Li}_2\text{CO}_3$ (technical grade) is dissolved at low temperatures and re-heated to produce $\text{Li}_2\text{CO}_3$ (battery grade).
Salar de Olaroz, Argentina (12 000 t $\text{Li}_2\text{CO}_3$ )	The pumped brine first reacts with quicklime and is then enriched from 0.06 wt. % Li to 1.2 wt. % Li in the evaporation ponds. In the processing

	<p>plant, the brine reacts with soda ash to let impure <math>\text{Li}_2\text{CO}_3</math> precipitate (Ehren and De Castro Alem, 2018; Orocobre, 2019). Then, <math>\text{Li}_2\text{CO}_3</math> is dissolved in deionized water at low temperatures and the solution is sent through ion exchangers to remove residual Mg, Ca, and B. To precipitate <math>\text{Li}_2\text{CO}_3</math> (battery grade), the pulp is re-heated as a last step (Ehren and De Castro Alem, 2018).</p>
<p>Salar de Cauchari-Olaroz, Argentina (40 000 t <math>\text{Li}_2\text{CO}_3</math>)</p>	<p>The pumped brine is enriched from 0.05 wt. % until 4 wt. % Li in evaporation ponds. Quicklime is added to remove Mg (Tran and Luong, 2015). B is removed via organic solvent extraction followed by removing Mg and Ca salts by adding quicklime and soda ash (Perez et al., 2014). The pulp is then heated to remove residual sulfates (Andeburg Consulting Services Inc and Montgomery &amp; Associates, 2019). An evaporator is then used to decrease the volume of the Li-containing pulp, which is followed by an ion exchanger to remove any residual impurities (Andeburg Consulting Services Inc and Montgomery &amp; Associates, 2019). In the next step, <math>\text{Li}_2\text{CO}_3</math> (technical grade) is forced to precipitate by heating the pulp and adding soda ash. Subsequently, <math>\text{Li}_2\text{CO}_3</math> is dissolved in water at low temperatures, and the solution is re-heated to produce <math>\text{Li}_2\text{CO}_3</math> (battery grade) (Perez et al., 2014).</p>
<p>Salar del Hombre Muerto (North), Argentina (5 000 t <math>\text{Li}_2\text{CO}_3</math>)</p>	<p>A processing sequence similar to Salar de Atacama has been suggested (Knight Piésold Ltd. and JDS Energy &amp; Mining Inc., 2019). As a first step, the brine would be enriched from 0.07 wt. % Li until 4 wt. % Li in evaporation ponds. Quicklime would be added to the evaporation ponds (Knight Piésold Ltd. and JDS Energy &amp; Mining Inc., 2019). In the processing plant, purification steps would consist of B removal by organic</p>

	<p>solvent extraction, Mg and Ca removal by adding soda ash and quicklime. Then, <math>\text{Li}_2\text{CO}_3</math> (technical grade) precipitates by heating the pulp and adding soda ash. <math>\text{Li}_2\text{CO}_3</math> (technical grade) is then dissolved in water at low temperatures and re-heated to precipitate <math>\text{Li}_2\text{CO}_3</math> (battery grade).</p>
<p>Chaerhan salt lake, China (8 000 t <math>\text{Li}_2\text{CO}_3</math>)</p>	<p>This <math>\text{Li}_2\text{CO}_3</math> production plant uses the residual K-depleted pulp of a K fertilizers production plant. This pulp contains 0.022 wt. % Li (Lanke Lithium, 2018). The first step is a Li-adsorption technique, where alumina hydroxide is used as a resin to adsorb Li selectively. Deionized water is used to remove Li from the adsorbent again. The Li-containing solution is sent through ion exchangers to remove still existing impurities. Nanofiltration and reverse osmosis are then required to reduce the volume of the Li-containing solution (Wen et al., 2006). Solar evaporation continuously reduces the brine volume from which subsequently <math>\text{Li}_2\text{CO}_3</math> (technical grade) is produced (Gansu United testing services Co Ltd, 2018; Lanke Lithium, 2018; Li et al., 2020). Due to the aforementioned required system expansion, we added the process sequence for <math>\text{Li}_2\text{CO}_3</math> (battery grade).</p>

197

198       **(2) Process-specific modeling of material and energy demands**

199       The resource demand of each process was calculated based on mass and energy balances as proposed by

200       our approach. We calculated the mass required in the evaporation ponds to produce 1 kg  $\text{Li}_2\text{CO}_3$  (battery

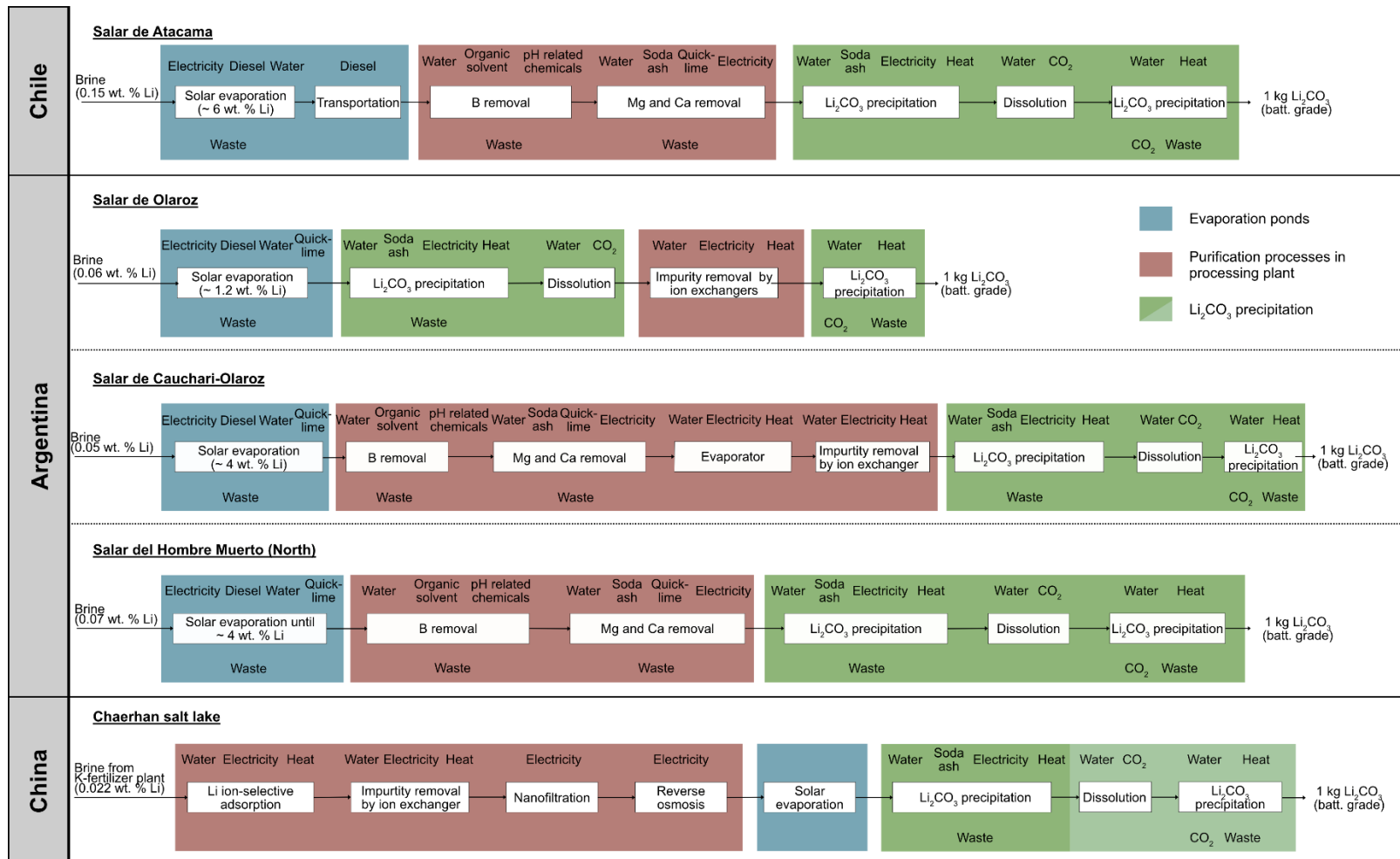
201       grade) based on the reported Li concentration of the brine. For the evaporation ponds, waste production is

202       not considered because the wastes from the different sites consist mainly of precipitated salts discarded in

203       the near-by salt flats and are thus expected to have limited environmental impacts for the covered types of

204       impact categories. The Li concentration of the enriched brine then served as an approximation of the mass

205 going into the processing plant. Based on the calculated mass flow, chemicals were estimated based on  
206 stoichiometries. To account for the incompleteness of the chemical reaction, 20 % mass is added to the  
207 modeled quicklime consumption based on Flexer et al. (2018) and 10 % to the modeled soda ash  
208 consumption (Li et al., 2020). 98.5 % of the organic solvent required in the B removal step is assumed to  
209 be recycled (CELIMIN, personal communication). Since deionized water is required in various processes,  
210 we estimated the required mass of water for each process. The brine operators reported water purification  
211 steps. However, they are not explicitly stated. Hence, for all brine operations we assumed that brackish  
212 water is treated by a reverse osmosis and an ion exchanger at all salt lakes (e.g., Lithium Americas Corp.  
213 2019). Due to the lack of site-specific information regarding waste treatment at the processing plants, we  
214 did not include waste treatment in the LCI, in contrast to the existing dataset in ecoinvent v3.8 (ecoinvent  
215 2021). Sources of thermal and electrical energy (i.e., heat from natural gas, heat and power co-generation  
216 from natural gas, and power from the location-specific grid) were based on company reports. Efficiencies  
217 of thermal processes are assumed to be 85 % due to the lack of information in used literature (U.S.  
218 Department of Energy Energy Efficiency and Renewable Energy, 2003).



219

220 Figure 2 Process sequence of the five brine sites. The blue squares indicate that the processes are related to evaporation ponds, while red squares represent  
 221 purification steps in the processing plant. Green squares represent Li<sub>2</sub>CO<sub>3</sub> precipitation steps. Bright green squares within the processing sequence of Chaerhan  
 222 salt lake indicate the required system expansion.

223 **Modeled resource consumption**

224 Table 2 presents the modeled inputs per kg Li<sub>2</sub>CO<sub>3</sub> (battery grade) from the five sites. We find that Chaerhan  
 225 salt lake has the highest consumption in electricity (27.8 kWh/kg Li<sub>2</sub>CO<sub>3</sub>), heat (298 MJ/kg Li<sub>2</sub>CO<sub>3</sub>), and  
 226 water (474 kg/kg Li<sub>2</sub>CO<sub>3</sub>) due to the specific Li-ion adsorption, ion exchangers and the following  
 227 nanofiltration, respectively reverse osmosis used for purification. Water (219 kg/kg Li<sub>2</sub>CO<sub>3</sub>) and electricity  
 228 (1.5 kWh/kg Li<sub>2</sub>CO<sub>3</sub>) demand at Salar de Olaroz are higher than the other South American salt lakes. The  
 229 water and electricity consumption originates from the intensive use of ion exchangers for removing  
 230 impurities and re-generating ion exchangers. Since Salar de Olaroz relies on removing impurities by ion  
 231 exchangers, Salar de Olaroz does not require any B removal-related chemicals in contrast to Salar de  
 232 Atacama, Salar de Cauchari-Olaroz, and Salar del Hombre Muerto (North). Quicklime demand in the  
 233 evaporation ponds to remove Mg is highest at Salar de Olaroz, while Salar de Atacama requires the lowest  
 234 quicklime demand per kg Li<sub>2</sub>CO<sub>3</sub>. At Salar de Atacama, quicklime is only required to remove residual Mg  
 235 from the pulp in the processing plant. Soda ash is used at all sites, mainly due to the Li<sub>2</sub>CO<sub>3</sub> precipitation  
 236 step.

237 *Table 2 Modeled life cycle inputs for 1 kg Li<sub>2</sub>CO<sub>3</sub> (battery grade) production at selected salt lakes.*

<b>Input demand/kg Li<sub>2</sub>CO<sub>3</sub></b>	<b>Salar de Atacama</b>	<b>Salar de Olaroz</b>	<b>Salar de Cauchari-Olaroz</b>	<b>Salar del Hombre Muerto</b>	<b>Chaerhan salt lake</b>
<i>Electricity [kWh]</i>	0.4	1.5	0.7	0.8	28
<i>Heat [MJ]</i>	19	19	28	14	298
<i>Water [kg]</i>	38	219	46	43	474
<i>Quicklime [kg]</i>	0.04	4.1	2.7	3.1	-
<i>Sodium hydroxide [kg]</i>	0.06	-	0.35	0.08	-
<i>Organic solvent [kg]</i>	0.04	-	0.1	0.7	-
<i>Hydrochloric acid [kg]</i>	0.10	-	0.5	0.9	-
<i>Soda ash [kg]</i>	1.9	1.6	2.1	1.6	1.6

238 **Step 3a: Life cycle impact assessment**

239 To assess environmental impacts of Li<sub>2</sub>CO<sub>3</sub> (battery grade) production from each salt lake, GWP 100a  
 240 (IPCC 2013), globally regionalized LCA impact assessment of PM formation (Oberschelp et al. 2020), and  
 241 partly regionalized WSF based on AWARE (Boulay et al., 2018) were chosen.

242 **Climate change impacts**

243 Figure 4-A presents the climate change impacts to produce 1 kg  $\text{Li}_2\text{CO}_3$  (battery grade) and their causes. In  
244 addition, we compare our results with two datasets (for  $\text{Li}_2\text{CO}_3$  from brines and spodumene-bearing  
245 pegmatites) provided in ecoinvent v3.8 (ecoinvent, 2021).

246 We find that  $\text{Li}_2\text{CO}_3$  production from the Salar de Atacama has the lowest climate change impacts (3.4 kg  
247  $\text{CO}_2\text{eq/kg Li}_2\text{CO}_3$ ). Heat (41 % of the climate change impacts) and on-site chemicals use (38 %) are the  
248 predominant contributors to the overall impacts. Soda ash for  $\text{Li}_2\text{CO}_3$  precipitation is responsible for 31 %  
249 of the total climate change impacts, while other chemicals, like organic solvents, quicklime, and  
250 hydrochloric acid, only contribute minor shares. Hence, we find that  $\text{Li}_2\text{CO}_3$  (technical grade) precipitation  
251 followed by  $\text{Li}_2\text{CO}_3$  (battery grade) precipitation are the major processes contributing to climate change per  
252 kg  $\text{Li}_2\text{CO}_3$  (battery grade) at Salar de Atacama (Figure 3). This is also in accordance with the findings by  
253 Stamp et al. (2012) and Kelly et al. (2021) when assessing environmental impacts related to the  $\text{Li}_2\text{CO}_3$   
254 production at the Salar de Atacama.

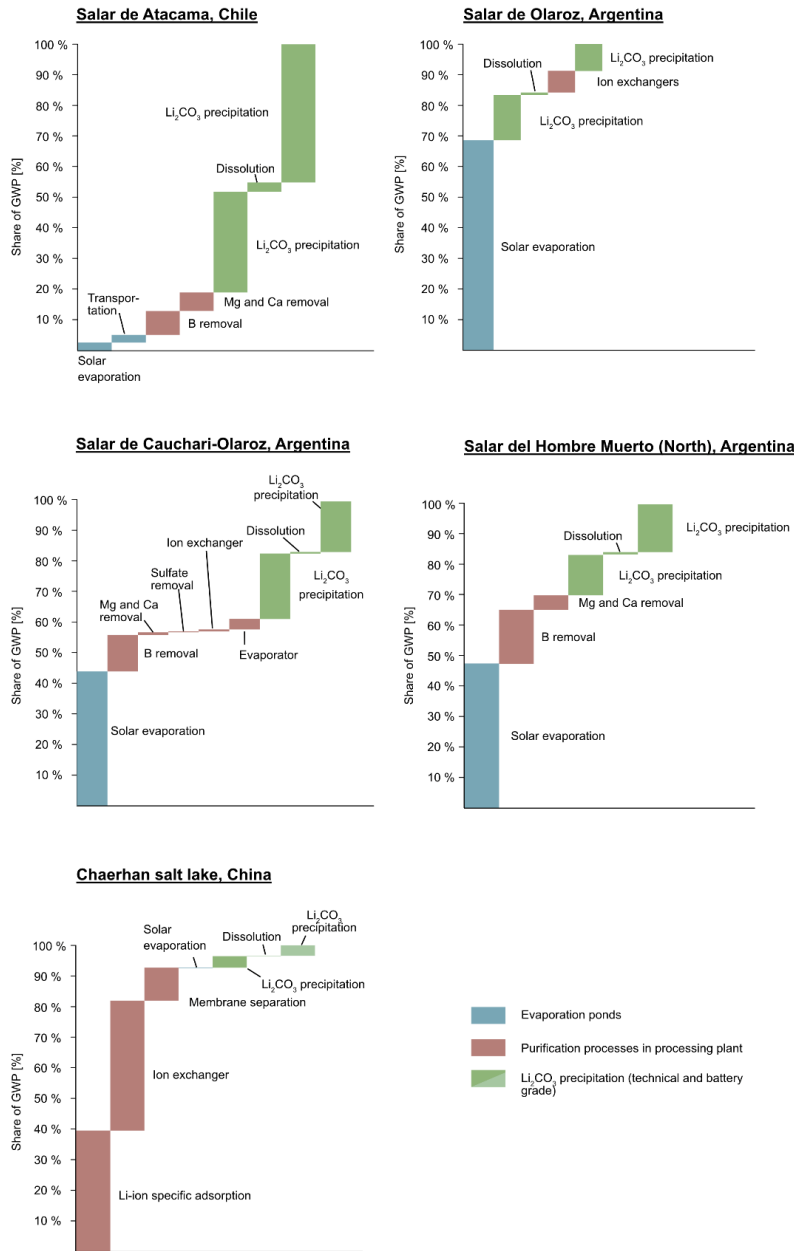
255 Climate change impacts related to the Argentinian brines are up to 235 % higher than for  $\text{Li}_2\text{CO}_3$  extracted  
256 from the Salar de Atacama (Salar de Olaroz: 7.4 kg  $\text{CO}_2\text{eq/kg Li}_2\text{CO}_3$ ; Salar de Cauchari-Olaroz: 7.7 kg  
257  $\text{CO}_2\text{eq/kg Li}_2\text{CO}_3$ ; Salar del Hombre Muerto (North): 8 kg  $\text{CO}_2\text{eq/kg Li}_2\text{CO}_3$ ). Quicklime required in the  
258 evaporation ponds to remove impurities contributes to the total climate change impacts (Salar de Olaroz:  
259 67 % of the total impact; Salar de Cauchari-Olaroz: 43 %; Salar del Hombre Muerto (North): 49 %), while  
260 heat and electricity on-site contribute to a minor extent. Quicklime production, in general, is associated  
261 with significant GHG emissions (Eula 2014). First, the production is heavily energy-intensive and mainly  
262 based on fossil fuels. Second, the chemical reaction to produce quicklime from limestone emits  $\text{CO}_2$  as a  
263 co-product (European Lime Association, 2014). Those two factors are reflected in the overall impacts if  
264 quicklime is used in these evaporation ponds (Figures 3 and 4-A). Hence, evaporation ponds and  $\text{Li}_2\text{CO}_3$   
265 (technical grade) precipitation are the most critical contributors due to the usage of quicklime, respectively

266 soda ash for the Argentinian salt lakes. At Salar del Hombre Muerto (North) and Salar de Cauchari-Olaroz  
267 specifically, the B removal step additionally makes up a significant share of climate change impacts.

268 We find that  $\text{Li}_2\text{CO}_3$  from Chaerhan salt lake has by far the highest climate change impacts (31.6 kg  
269  $\text{CO}_2\text{eq/kg Li}_2\text{CO}_3$ ) resulting from the heat and electricity demand for the Li-ion selective adsorption  
270 technique. This technique mainly includes two phases (adsorption and desorption phase) which require the  
271 solution being heated up to a specific temperature using natural gas. Furthermore, electricity from the  
272 provincial electricity grid is required for the ion exchangers and membrane separation (nanofiltration and  
273 reverse osmosis) to remove impurities in the  $\text{Li}_2\text{CO}_3$  bearing solution.

274 Climate change impacts of  $\text{Li}_2\text{CO}_3$  from brines in ecoinvent v3.8 (2.1 kg  $\text{CO}_2\text{eq/kg Li}_2\text{CO}_3$ ) and a recent  
275 study by Kelly et al. (2021) (2.7 – 3.1 kg  $\text{CO}_2\text{eq/kg Li}_2\text{CO}_3$ ) are in the same range as the ones of our modeled  
276 LCI for Salar de Atacama. However, these numbers are lower than the other brines in Argentina and China,  
277 underestimating the climate change impacts of average  $\text{Li}_2\text{CO}_3$ . If  $\text{Li}_2\text{CO}_3$  is extracted from spodumene-  
278 bearing pegmatites, as described with the dataset provided by ecoinvent v3.8 (ecoinvent, 2021), the climate  
279 change impacts add up to 10.7 kg  $\text{CO}_2\text{eq/kg Li}_2\text{CO}_3$ . Kelly et al. (2021) estimated 20.4 kg  $\text{CO}_2\text{eq/kg Li}_2\text{CO}_3$   
280 from the Australian pegmatitic mine. Both estimations are higher than our results for the Argentinian salt  
281 lakes but still lower than the one for Chaerhan salt lake.

282



283

284 *Figure 3 Process-related contributive analyses regarding climate change impacts assessed with GWP (100 years)*  
 285 *shown in percentage. The blue squares indicate that the processes are related to evaporation ponds, while red squares*  
 286 *represent purification steps in the processing plant. Green squares indicate  $\text{Li}_2\text{CO}_3$  precipitation steps. Bright green*  
 287 *squares within the processing sequence of Chaerhan salt lake indicate that processes were added to hypothetically*  
 288 *produce  $\text{Li}_2\text{CO}_3$  (battery grade) to provide the same functional unit as the other systems.*

289 **PM-related human health impacts**

290 The results indicate a large variability in PM-related health impacts (Figure 4-B), which underlines the  
291 necessity to perform regionalized LCAs for brine operations in this impact category. The highest PM health  
292 impacts occur due to the  $\text{Li}_2\text{CO}_3$  production at Chaerhan salt lake (1.2 micro-disability adjusted life years  
293 ( $\mu\text{DALY}$ )/kg  $\text{Li}_2\text{CO}_3$ ) followed by Salar del Hombre Muerto (0.67  $\mu\text{DALY}$ /kg), Salar de Cauchari-Olaroz  
294 (0.67  $\mu\text{DALY}$ /kg), Salar de Atacama (0.43  $\mu\text{DALY}$ /kg), and Salar de Olaroz (0.31  $\mu\text{DALY}$ /kg). For all  
295 sites, the background processes predominantly contribute to PM health impacts in contrast to foreground  
296 processes (i.e., heat or diesel consumption) from the remote location of all salt lakes and low local  
297 population densities. Electricity use in China, India, and Indonesia for various products and services in the  
298 background system makes up a significant share of the overall impacts of all brine sites (Salar de Atacama:  
299 31 %; Salar de Olaroz: 44 %; Salar de Cauchari-Olaroz and Salar del Hombre Muerto (North): 56 %;  
300 Chaerhan salt lake: 48 %). The contribution of electricity required or generated on-site varies largely for  
301 PM health impacts. While the Argentinian electricity mix contributes to the overall PM health impacts with  
302 less than 1 %, the Chilean and Chinese electricity mix significantly contribute (27 % and 17 %) due to  
303 particulates,  $< 2.5 \mu\text{m}$ , sulfur dioxide, and nitrogen oxides from coal power generation. 43 % of the Chilean  
304 electricity mix comes from coal power. The Qinghai province-specific electricity mix, which was chosen  
305 for Chaerhan salt lake, consists of 22 % coal power, while the main source in this region is hydropower. In  
306 contrast, the Argentinian electricity mix includes little coal power (1 %) and does not significantly  
307 contribute to the PM health impacts.

308 Soda ash is a relevant contributor to the PM health impacts at all sites. The specific contributions range  
309 from 4 % at Chaerhan salt lake to 16 % at Salar de Atacama. During soda ash production, ammonia is  
310 released into the atmosphere contributing significantly to PM health impacts in highly populated areas, such  
311 as Europe. However, the location of soda ash production is highly uncertain since our results rather reflect  
312 the LCI in ecoinvent v3.8 than the actual resource supplier due to missing operational data.

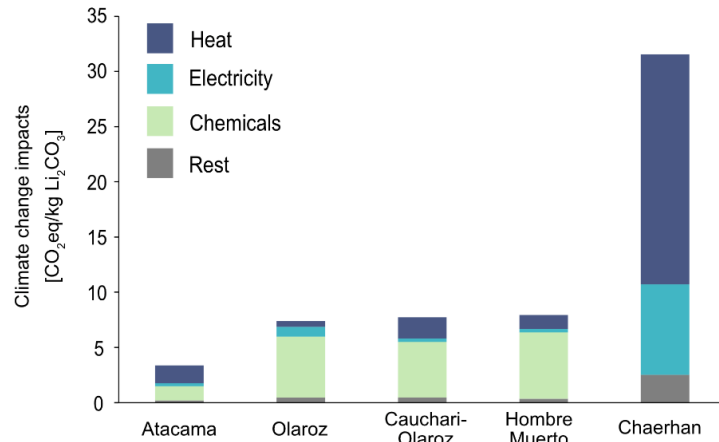
## 313 **Water scarcity footprint**

314 The WSF for each salt lake using the AWARE method (Boulay et al., 2018) is presented in Figure 4-C.  
315 Chaerhan salt lake has the highest impact on water scarcity ( $35.25 \text{ m}^3_{\text{world eq}}/\text{kg Li}_2\text{CO}_3$ ), followed by Salar  
316 de Atacama ( $4.77 \text{ m}^3_{\text{world eq}}/\text{kg Li}_2\text{CO}_3$ ). The Argentinian salt lakes are in the same range ( $1.36 \text{ m}^3_{\text{world eq}}/\text{kg}$   
317  $\text{Li}_2\text{CO}_3$  at Salar del Hombre Muerto,  $1.62 \text{ m}^3_{\text{world eq}}/\text{kg Li}_2\text{CO}_3$  at Salar de Cauchari-Olaroz, and  $1.73 \text{ m}^3_{\text{world}}$   
318  $\text{eq}/\text{kg Li}_2\text{CO}_3$  at Salar de Olaroz). The water scarcity impacts of Salar de Atacama predominately originate  
319 from the direct use of freshwater at the processing plant (81 %). However, Salar de Atacama has the lowest  
320 water demand on-site compared to all other salt lakes. Nevertheless, due to its high aridity (e.g., Munk et  
321 al. (2016)) the location-specific characterization factor is the highest with  $94.7 \text{ m}^3_{\text{world eq}}/\text{m}^3$  amongst these  
322 salt lakes, which is reflected in the overall water scarcity impacts.

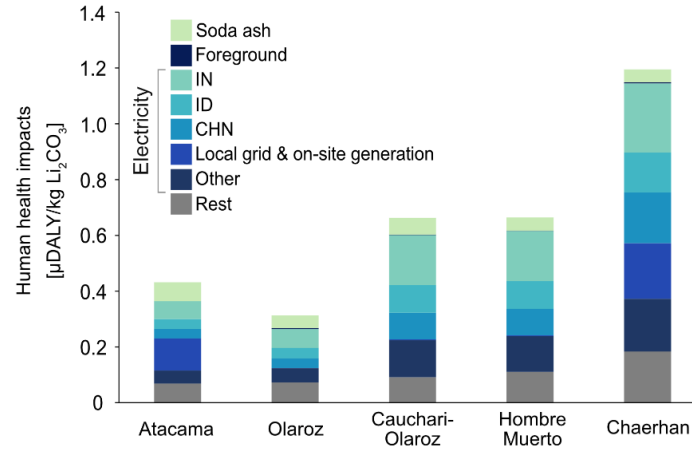
323 The Argentinian brines have the lowest WSF due to their relatively low characterization factor ( $2.7 - 5$   
324  $\text{m}^3_{\text{world eq}}/\text{m}^3$ ). This is particularly important for  $\text{Li}_2\text{CO}_3$  production at Salar de Olaroz, which has a high  
325 water requirement due to the intensive use of ion exchangers in the foreground system. The water demand  
326 originates from the regeneration of the resin used to remove residual impurities and then allow a  $\text{Li}_2\text{CO}_3$   
327 (battery grade) precipitation. Nevertheless, the overall impact is lower than the one from Salar de Atacama.  
328 In contrast to Salar de Olaroz, water scarcity impacts in the foreground are minor compared to the ones in  
329 the background at Salar de Cauchari-Olaroz (85 %) and Salar del Hombre Muerto (North) (91 %).

330 The WSF from  $\text{Li}_2\text{CO}_3$  production at Chaerhan salt lake originates from the extensive water use (see chapter  
331 resource consumption) in the processing plant due to the Li-ion specific adsorption technique. Furthermore,  
332 the location-specific characterization factor ( $70.6 \text{ m}^3_{\text{world eq}}/\text{m}^3$ ) contributes to the relatively high WSF. The  
333 water demand in the background only accounts for 5 % of the total WSF. In general, it has to be noted that  
334 the background water consumption was not allocated to specific regions and was assessed with the global  
335 average AWARE characterization factor, which is rather high (Boulay et al., 2018). Therefore, background  
336 water stress might be overestimated in some cases.

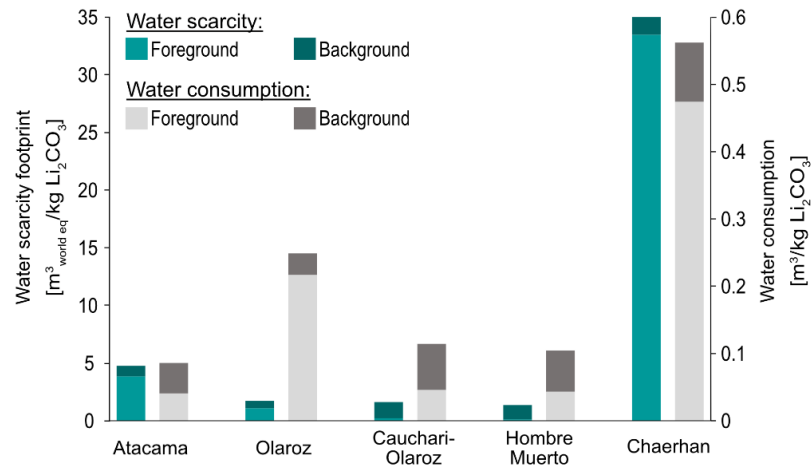
### A. Climate change impacts



### B. PM-related human health impacts



### C. Water scarcity footprint



337

338 Figure 4 Environmental impacts of Li<sub>2</sub>CO<sub>3</sub> production from brines. (A) Impacts on climate change (GWP 100 yrs), (B) PM-related human health impacts and

339 (C) WSF (primary y-axis), and water consumption (secondary y-axis). (A) and (C) are shown on a midpoint level and (B) on an endpoint level.

### 340 **Step 3b: Robustness and limitations of the approach**

341 We ran Monte Carlo simulations with  $n = 5000$  runs for the foreground system of each salt lake using GWP  
342 (IPCC 2013) and PM health impacts (Oberschelp et al. 2020) to assess the robustness of our results (more  
343 information in the SI). The relative standard deviation ranges from  $\pm 33\%$  (Salar de Atacama) to  $\pm 98\%$   
344 (Chaerhan salt lake) for impacts on climate change, while the Argentinian salt lakes are in-between. For  
345 PM-related health impacts, the relative standard deviation lies between  $\pm 46\%$  (Salar de Cauchari-Olaroz  
346 and Salar del Hombre Muerto (North)) and  $\pm 73\%$  (Chaerhan salt lake). The relatively higher standard  
347 deviation of Chaerhan salt lake is explained by the lowest data quality of all assessed sites. In general, the  
348 origin of inputs is mostly unknown, thus contributing to the uncertainties. We, therefore, relied onecoinvent  
349 data. In order to decrease these uncertainties, site-specific information regarding the input supply is crucial.  
350 If these data are not available, country-specific trading data could be obtained to decrease the uncertainties  
351 in the future.

352 There are also data gaps in our modeling approach which need to be discussed. Energy, water, and chemical  
353 demand modeled for this study were compared with annually reported company data or technical reports  
354 from exploration activity (more information in SI). We used company data as an indicator rather than as a  
355 fixed reference because specific boundaries and further documentation were generally not provided.  
356 Quantitative chemical demand at Salar de Cauchari-Olaroz has not been reported to the authors' knowledge  
357 and thus, could not be compared with our results. Furthermore, the LCI modeling of  $\text{Li}_2\text{CO}_3$  (battery grade)  
358 from Chaerhan salt lake predominately relies on parameters reported in construction plans by Gansu United  
359 testing services Co Ltd (2018), impeding to test robustness of the model for that site. Annual changes of  
360 the brine chemistry are challenging to include in the LCI, but may affect resource consumption (especially  
361 chemical and heating demand) on-site. We could not estimate the salt crystallization sequence and hence,  
362 calculate waste production in evaporation ponds. However, these wastes are mainly deposited on-site,  
363 requiring little transport.

## 364 **3.2 Implications for Li-ion battery production**

365 To set this study into a broader context, modelled LCIs of two brine sites (Chaerhan salt lake and Salar de  
366 Atacama) were implemented in an ecoinvent v3.8 dataset, which represents the production of 1 kg  
367 rechargeable Li-ion batteries. This type of battery is used for a variety of electrical vehicles (Crenna et al.,  
368 2021). Furthermore, we also adjusted the ecoinvent dataset to only use Li from the brine dataset in ecoinvent  
369 v3.8. This leads to three battery datasets:

- 370 1. 100 % of the  $\text{Li}_2\text{CO}_3$  production originates from the dataset for  $\text{Li}_2\text{CO}_3$  from brines in ecoinvent  
371 v3.8 (based on Salar de Atacama).
- 372 2. 100 % of the entire  $\text{Li}_2\text{CO}_3$  production is assumed to be from Salar de Atacama.
- 373 3. 100 % of the entire  $\text{Li}_2\text{CO}_3$  production is replaced by  $\text{Li}_2\text{CO}_3$  from Chaerhan salt lake.

374 As already Stamp et al. (2012) and Kelly et al. (2021) highlighted, the source of lithium affects the amount  
375 of GHG emissions related to Li-ion battery production. The maximum increase of climate change impacts  
376 is 19 % when implementing 100 %  $\text{Li}_2\text{CO}_3$  production by Chaerhan salt lake (dataset 3) compared to the  
377 baseline (dataset 1). The leading cause is the high thermal and electrical energy demand based on fossil  
378 fuels of Chaerhan salt lake.  $\text{Li}_2\text{CO}_3$  from Salar de Atacama (dataset 2) only increases climate change impact  
379 of a Li-ion battery by < 1 %. In the future, more lithium production might be sourced from high-impact  
380 mines since an increase in demand and price might make energy-intense production routes profitable.  
381 Multiple studies emphasize the range of reported or modeled GHG emissions related to Li-ion battery  
382 production (e.g., Raugei and Winfield 2019; Crenna et al. 2021). For our study, these findings indicate that  
383 the overall share of  $\text{Li}_2\text{CO}_3$  from brines regarding impacts may change in the future due to more detailed  
384 and transparent Li-ion battery supply chains. Thus, LCA and carbon footprinting of future battery  
385 production should consider the potential for high-impact  $\text{Li}_2\text{CO}_3$  supply and consider the existing LCIs as  
386 highly uncertain.

## 387 **4 Conclusion and outlook**

388 The Li supply is key for the transition towards a global decarbonized society. Li expects higher growth  
389 rates than other metals in the future. Hence, it is inevitable to assess environmental impacts of current and  
390 future Li extraction to avoid severe environmental burden shifting. Currently used LCIs of  $\text{Li}_2\text{CO}_3$  from  
391 brines do not represent the global market nowadays and even less for the future. Thus, we developed a  
392 framework to update LCIs of  $\text{Li}_2\text{CO}_3$  production from brines site-specifically. This methodology was  
393 applied to existing and future production sites. Our framework helps to treat data gaps and to derive process-  
394 specific parameters from patents. Furthermore, an approach to assess sites using waste streams as a Li  
395 source, like Chaerhan salt lake, was developed. Regionalization of foreground and background data as well  
396 as using regionalized impact assessment methods were examined and discussed in detail. Our results  
397 demonstrate the necessity of defining a framework to assess various sites and resulting variabilities in global  
398 production. The case studies show that available literature data underestimate environmental impacts of  
399  $\text{Li}_2\text{CO}_3$  production from brines. This mainly is a consequence of only assessing  $\text{Li}_2\text{CO}_3$  production at Salar  
400 de Atacama and assuming that this data is representative of  $\text{Li}_2\text{CO}_3$  production in general, which is not the  
401 case. Furthermore, the variability of our results is a consequence of the brine composition, the applied  
402 processing technique, and the brine location. For instance, water scarcity and PM impacts need to be site-  
403 specifically assessed since the location of impact (background or foreground) varies among these sites.  
404 Future improvements regarding the assessment of Li should focus on other Li sources, such as pegmatites,  
405 geothermal brines, and seawater.

406 The integration of obtained LCIs in Li-ion batteries demonstrates that the overall impacts on climate change  
407 increase to up to 19%. Hence, supply chains of Li-ion batteries need to be assessed in detail, especially for  
408 future scenarios. Improvements regarding the resolution of supply chains are crucial to transition towards  
409 low-carbon technologies sustainably. This includes site-specific assessment of other minerals for batteries  
410 like Aluminum and Cobalt, such as recently done for copper mine tailings (Adrianto et al., 2022). Our  
411 framework serves as a starting point for enhancing LCI and regionalized LCIA of other battery minerals.

412 **Acknowledgments**

413 The authors would like to thank Stefanie Hellweg for insightful discussions and internal review. The authors  
414 would like to thank Leonard Zourek, Lu Meng, and Qinhan Zhu for collecting data. The authors further  
415 thank Mario Grágeda Zegarra and Alonso Gonzalez from the Centro de investigación avanzada del litio y  
416 minerales industriales for sharing their knowledge. The authors also thank Aleksandra Kim for supporting  
417 with Brightway2. The authors further thank Maja Wiprächtiger for internal review and Mary Graybeal for  
418 proofreading the paper. This work was done within the project “e-Bike City”. Funding by the Civil,  
419 Geomatics, and Environmental Engineering Department of ETH Zürich is gratefully acknowledged. This  
420 publication was created as part of NCCR Catalysis, a National Centre of Competence in Research funded  
421 by the Swiss National Science Foundation.

422 **Declaration of interest**

423 The authors declare no competing interests.

424

## 425 **Bibliography**

- 426 Adrianto, L.R., Pfister, S., Hellweg, S., 2022. Regionalized Life Cycle Inventories of Global Sulfidic  
427 Copper Tailings. *Environ. Sci. Technol.* <https://doi.org/10.1021/acs.est.1c01786>
- 428 Ambrose, H., Kendall, A., 2019. Understanding the future of lithium: Part 2, temporally and spatially  
429 resolved life-cycle assessment modeling. *J. Ind. Ecol.* 1–11. <https://doi.org/10.1111/jiec.12942>
- 430 Andeburg Consulting Services Inc, Montgomery & Associates, 2019. Updated Feasibility Study and  
431 Mineral Reserve Estimation to Support 40,000 tpa Lithium Carbonate Production at the Cauchari-  
432 Olaroz Salars, Jujuy Province, Argentina.
- 433 Bertau, M., Voigt, W., Schneider, A., Martin, G., 2017. Lithium Recovery from Challenging Deposits:  
434 Zinnwaldite and Magnesium-Rich Salt Lake Brines. *Chemie-Ingenieur-Technik* 89, 64–81.  
435 <https://doi.org/10.1002/cite.201600101>
- 436 Boulay, A.-M., Bare, J., Benini, L., Berger, M., Lathuillière, M.J., Manzardo, A., Margni, M., Motoshita,  
437 M., Núñez, M., Pastor, A.V., Ridoutt, B., Oki, T., Worbe, S., Pfister, S., 2018. The WULCA consensus  
438 characterization model for water scarcity footprints: assessing impacts of water consumption based  
439 on available water remaining (AWARE). *Int. J. Life Cycle Assess.* 23, 368–378.  
440 <https://doi.org/10.1007/s11367-017-1333-8>
- 441 Christmann, P., Gloaguen, E., Labbé, J.-F., Melleton, J., Piantone, P., 2015. Global Lithium Resources  
442 and Sustainability Issues, in: *Lithium Process Chemistry*. Elsevier, pp. 1–40.  
443 <https://doi.org/10.1016/b978-0-12-801417-2.00001-3>
- 444 Crenna, E., Gauch, M., Widmer, R., Wäger, P., Hischier, R., 2021. Towards more flexibility and  
445 transparency in life cycle inventories for Lithium-ion batteries. *Resour. Conserv. Recycl.* 170, 105619.  
446 <https://doi.org/10.1016/J.RESCONREC.2021.105619>
- 447 Dai, Q., Kelly, J.C., Dunn, J., Benavides, P.T., 2020. Update of Bill-of-Materials and Cathode Chemistry  
448 addition for Lithium-ion Batteries in GREET Model.
- 449 ecoinvent, 2021. ecoinvent v3.8 database (cut-off version).
- 450 Ehren, P., De Castro Alem, J., 2018. Process for producing lithium carbonate from concentrated lithium  
451 brine.
- 452 European Lime Association, 2014. A competitive and efficient lime industry.

453 Flexer, V., Baspineiro, C.F., Galli, C.I., 2018. Lithium recovery from brines: A vital raw material for green  
454 energies with a potential environmental impact in its mining and processing. *Sci. Total Environ.*  
455 <https://doi.org/10.1016/j.scitotenv.2018.05.223>

456 Gansu United testing services Co Ltd, 2018. Environmental impact acceptance certificate of Lanke Lithium  
457 10000 ton upgrade construction project.

458 Garrett, D.E., 2004. Handbook of lithium and natural calcium chloride : their deposits, processing, uses and  
459 properties , 1st ed. ed. Elsevier Academic Press, Amsterdam ;

460 Houston, J., Butcher, A., Ehren, P., Evans, K., Godfrey, L., 2011. The evaluation of brine prospects and the  
461 requirement for modifications to filing standards. *Econ. Geol.* 106, 1125–1239.  
462 <https://doi.org/10.2113/econgeo.106.7.1225>

463 ISO, 2006a. ISO 14040:2006 Environmental management - Life cycle assessment - Principles and  
464 framework.

465 ISO, 2006b. ISO 14044:2006 Environmental management - Life cycle assessment - Requirements and  
466 guidelines.

467 Jiang, S., Zhang, L., Li, F., Hua, H., Liu, X., Yuan, Z., Wu, H., 2020. Environmental impacts of lithium  
468 production showing the importance of primary data of upstream process in life-cycle assessment. *J.*  
469 *Environ. Manage.* 262, 110253. <https://doi.org/10.1016/j.jenvman.2020.110253>

470 Kelly, J.C., Wang, M., Dai, Q., Winjobi, O., 2021. Energy, greenhouse gas, and water life cycle analysis of  
471 lithium carbonate and lithium hydroxide monohydrate from brine and ore resources and their use in  
472 lithium ion battery cathodes and lithium ion batteries. *Resour. Conserv. Recycl.* 174, 105762.  
473 <https://doi.org/10.1016/J.RESCONREC.2021.105762>

474 Kesler, S.E., Gruber, P.W., Medina, P.A., Keoleian, G.A., Everson, M.P., Wallington, T.J., 2012. Global  
475 lithium resources: Relative importance of pegmatite, brine and other deposits. *Ore Geol. Rev.*  
476 <https://doi.org/10.1016/j.oregeorev.2012.05.006>

477 Knight Piésold Ltd., JDS Energy & Mining Inc., 2019. NI 43-101 PRELIMINARY ECONOMIC  
478 ASSESSMENT REPORT for the HOMBRE MUERTO NORTE PROJECT SALTA PROVINCE,  
479 ARGENTINA.

480 Lanke Lithium, 2018. Chemical design plan of Lanke Lithium 10000 ton upgrade construction project.

481 Li, B., Wu, J., Lu, J., 2020. Life cycle assessment considering water-energy nexus for lithium nanofiltration

482 extraction technique. *J. Clean. Prod.* 261, 121152. <https://doi.org/10.1016/j.jclepro.2020.121152>

483 Liu, W., Agusdinata, D.B., 2021. Dynamics of local impacts in low-carbon transition: Agent-based  
484 modeling of lithium mining-community-aquifer interactions in Salar de Atacama, Chile. *Extr. Ind.*  
485 *Soc.* 100927. <https://doi.org/10.1016/J.EXIS.2021.100927>

486 Liu, W., Agusdinata, D.B., Myint, S.W., 2019. Spatiotemporal patterns of lithium mining and  
487 environmental degradation in the Atacama Salt Flat, Chile. *Int. J. Appl. Earth Obs. Geoinf.* 80, 145–  
488 156. <https://doi.org/10.1016/J.JAG.2019.04.016>

489 Marazuela, M.A., Vázquez-Suñé, E., Ayora, C., García-Gil, A., 2019. Towards more sustainable brine  
490 extraction in salt flats: Learning from the Salar de Atacama. *Sci. Total Environ.*  
491 <https://doi.org/10.1016/j.scitotenv.2019.135605>

492 Munk, L.A., Hynek, S.A., Bradley, D., Boutt, D.F., Labay, K., Jochens, H., 2016. Lithium brines: A global  
493 perspective. *Rev. Econ. Geol.* 18, 339–365.

494 Mutel, C., 2017. Brightway: An open source framework for Life Cycle Assessment. *J. Open Source Softw.*  
495 2, 236. <https://doi.org/10.21105/JOSS.00236>

496 Oberschelp, C., Pfister, S., Hellweg, S., 2020. Globally Regionalized Monthly Life Cycle Impact  
497 Assessment of Particulate Matter. *Environ. Sci. Technol.* 54, 16028–16038.  
498 <https://doi.org/10.1021/acs.est.0c05691>

499 Oberschelp, C., Pfister, S., Raptis, C.E., Hellweg, S., 2019. Global emission hotspots of coal power  
500 generation. *Nat. Sustain.* 2, 113–121. <https://doi.org/10.1038/s41893-019-0221-6>

501 Orocobre, 2019. 2019 Sustainability full report.

502 Perez, W., Barrientos, H.A.C., Suarez, C., Bravo, M., 2014. Method for the production of battery grade  
503 lithium carbonate from natural and industrial brines.

504 Raugei, M., Winfield, P., 2019. Prospective LCA of the production and EoL recycling of a novel type of  
505 Li-ion battery for electric vehicles. *J. Clean. Prod.* 213, 926–932.  
506 <https://doi.org/10.1016/J.JCLEPRO.2018.12.237>

507 S&P Global, 2021. Market Intelligence - Metals & Mining Properties [WWW Document]. URL  
508 <https://www.spglobal.com/marketintelligence/en/>

509 Schomberg, A.C., Bringezu, S., Flörke, M., 2021. Extended life cycle assessment reveals the spatially-  
510 explicit water scarcity footprint of a lithium-ion battery storage. *Commun. Earth Environ.* 2, 11.

511 <https://doi.org/10.1038/s43247-020-00080-9>

512 Stamp, A., Lang, D.J., Wäger, P.A., 2012. Environmental impacts of a transition toward e-mobility: The  
513 present and future role of lithium carbonate production. *J. Clean. Prod.* 23, 104–112.  
514 <https://doi.org/10.1016/j.jclepro.2011.10.026>

515 Steubing, B., de Koning, D., Haas, A., Mutel, C.L., 2020. The Activity Browser — An open source LCA  
516 software building on top of the brightway framework. *Softw. Impacts* 3, 100012.  
517 <https://doi.org/10.1016/J.SIMPA.2019.100012>

518 Swain, B., 2017. Recovery and recycling of lithium: A review. *Sep. Purif. Technol.* 172, 388–403.  
519 <https://doi.org/10.1016/j.seppur.2016.08.031>

520 Tran, T., Luong, V.T., 2015. Lithium Production Processes, Lithium Process Chemistry: Resources,  
521 Extraction, Batteries, and Recycling. Elsevier Inc. [https://doi.org/10.1016/B978-0-12-801417-](https://doi.org/10.1016/B978-0-12-801417-2.00003-7)  
522 [2.00003-7](https://doi.org/10.1016/B978-0-12-801417-2.00003-7)

523 U.S. Department of Energy Energy Efficiency and Renewable Energy, 2003. A BestPractices Steam  
524 Technical Brief - How To Calculate The True Cost of Steam 13.

525 Wanger, T.C., 2011. The Lithium future-resources, recycling, and the environment. *Conserv. Lett.* 4, 202–  
526 206. <https://doi.org/10.1111/j.1755-263X.2011.00166.x>

527 Wen, X., Ma, P., Zhu, C., He, Q., Deng, X., 2006. Preliminary study on recovering lithium chloride from  
528 lithium-containing waters by nanofiltration. *Sep. Purif. Technol.* 49, 230–236.  
529 <https://doi.org/10.1016/j.seppur.2005.10.004>

530 Wernet, G., Bauer, C., Steubing, B., Reinhard, J., Moreno-Ruiz, E., Weidema, B., 2016. The ecoinvent  
531 database version 3 (part I): overview and methodology. *Int. J. Life Cycle Assess.* 21, 1218–1230.  
532 <https://doi.org/10.1007/s11367-016-1087-8>

533 Wilkomirsky, I., 1999. Production of lithium carbonate from brines.

534 World Economic Forum, 2019. A Vision for a Sustainable Battery Value Chain in 2030 Unlocking the Full  
535 Potential to Power Sustainable Development and Climate Change Mitigation.

536